Published in final edited form as:
Biochim Biophys Acta. 2007 April ; 1770(4): 694–705.

Ontogeny of *rdh9* (Crad3) expression: ablation causes changes in retinoid and steroid metabolizing enzymes, but RXR and androgen signaling seem normal

Peirong Hu, **Min Zhang**[1], and **Joseph L. Napoli**[2]
Department of Nutritional Science & Toxicology, University of California, Berkeley, CA 94720

Abstract

Crad3 (*cis*-retinol/androgen dehydrogenase 3), a short-chain dehydrogenase/reductase**,** converts 9-cis-retinol into 9-cis-retinal and 3α-androstanediol into dihydrotestosterone. Crad3 may serve in biosynthesis of 9-cis-retinoic acid, a putative RXR ligand, and/or regeneration of potent androgens. RT-PCR showed that expression of the gene that encodes Crad3, *rdh9*, begins in liver by e11.5, and in kidney, testis, brain and intestine during e15.5-e16.5. In situ hybridization showed *rdh9* expression in embryonic liver, ganglia, small intestine, lung, skin and vertebral cartilage. In adult, in situ hybridization revealed *rdh9* expression intensely in hepatocytes, weakly in kidney glomerulus, and intensely in collecting tubules. In intestine, undifferentiated epithelia had greater expression than differentiated epithelia at the distal villus end. Testes expressed *rdh9* in spermatogonia, and weakly in Leydig cells. Adult brain expressed *rdh9* in the dentate gyrus and CA regions of the hippocampus, the cerebellum purkinje cells, and the glomerular and mitral cell layers of the olfactory bulb. *Rdh9*-null mice, backcrossed against C57BL/6J mice, were born in Mendelian frequency, were healthy and fertile, and had normal tissue retinoid and serum dihydrotestosterone levels. Expression of *rdh1*, a gene that encodes an efficient retinol dehydrogenase, decreased 3 to 8-fold in *rdh9*-null mice, depending on dietary vitamin A. Microarray analysis and quantitative PCR revealed 2-4-fold increases in mRNA of enzymes that catalyze xenobiotic and steroid metabolism, including Cyp2, Cyp3, 11β-hydroxysteroid dehydrogenase type 2, and 17β-hydroxsteroid dehydrogenases types 4 and 5. These data indicate widespread Crad3 function(s) in steroid and/or retinoid metabolism starting mid embryogenesis.

Keywords

retinoic acid; dihydrotestosterone; short-chain dehydrogenase/reductase; androgen; hydroxysteroid dehydrogenase

1. Introduction

Several SDRs catalyze cis-retinoid dehydrogenation [1]. Among these, Crad3 catalyzes conversion of 9-cis-retinol into 9-cis-retinal most efficiently (highest Vm/K_m) [2]. Raldh1, 2, and 3 catalyze all-trans-retinal and 9-cis-retinal dehydrogenation, whereas Raldh4 has activity only with 9-cis-retinal [3–5]. Transfection of Crad3 into intact cells with any one of these Raldh

[1] Address reprint requests to: Joseph L. Napoli, 119 Morgan Hall, MC#3104, University of California, Berkeley, CA 94720, Phone: 510-642-5202, FAX: 510-642-0535, Email: jna@berkeley.edu
[2]Current address: Cell Sciences and Development, SAFC Biosciences, Sigma-Aldrich, St. Louis, MO 63103.

expresses enzymatic pathways that convert 9-cis-retinol into 9-cis-RA. Crad3 also has about equivalent enzymatic efficiency (Vm/K_m) for 3α-androstanediol dehydrogenation, but has no detectable activity with testosterone, DHT, estradiol (17β-HSD activity), or all-trans-retinol. Crad3, therefore, could function in vivo as a cis-retinoid dehydrogenase and/or a 3α-HSD.

The nuclear receptors RXRα, β and γ serve as obligatory heterodimeric partners for the nuclear receptors LXR, FXR, PPARα, β and γ, RARα, β and γ, TRα and β, and VDR [6,7]. Through effects on these diverse receptors, RXR contribute to regulating multiple distinct and often overlapping biological processes [8]. Despite the importance of RXR, the nature of its endogenous ligand(s), if any, remains uncertain. Two groups have concluded that 9-cis-RA serves as the endogenous RXR ligand [9,10]. 9-cis-RA, however, has not been detected in vivo, either by validated HPLC assays or by ultra sensitive LC tandem mass spectrometry assays [11,12]. Docosahexaenoic acid has been proposed as an endogenous RXR ligand [13]. Docosahexaenoic acid, however, binds RXR with a k_d ~200 μM, most likely far above the concentration available to nuclear receptors. Phytanic acid reportedly has a k_d value with RXRα ~4 μM, lower than its physiological concentration ~30 μM [14,15]. Neither docosahexaenoic acid nor phytanic acid have been associated with endogenous RXR in situ. A crystallized complex of the RXR and RAR ligand-binding domains contained oleic acid in the RXR binding pocket [16]. Nevertheless, no data indicate that dietary polyunsaturated fatty acids or phytols affect RXR signaling.

Although it seems reasonable to conclude that 9-cis-RA does not occur in vivo because it has not been detected, 9-cis-RA could have steady-state concentrations below current detection limits, resulting from rapid metabolism. Experimental observations are consistent with this notion. Fresh and processed fruits and vegetables contain both 9-cis-retinol and 9-cis-β-carotene [17–22]. A specific transporter facilitates intestinal uptake of all-trans-retinol, but uptake of 9-cis-retinol also occurs, probably through diffusion [23]. 9-cis-Retinol, 9-cis-β-carotene and 9-cis-RE have not been detected in serum, but accumulate in mammalian tissues, albeit at a fraction of the concentrations of all-trans-isomers [24–27]. 9-cis-RA dosed intramuscularly to rodents disappears rapidly from serum, followed by an increase in 9,13-di-cis-RA, a physiologically occurring retinoid [28–31]. Thus, 9-cis-retinoids and carotenoids occur in nature, cells express enzymes that recognize dietary 9-cis-retinoids as substrates, these enzymes generate 9-cis-RA in intact cells, and a 9-cis-RA metabolite occurs in vivo.

Here we report *rdh9* mRNA expression patterns during embryogenesis and in adult mouse tissues, and test function of Crad3 in vivo via generation of *rdh9*-null mice.

2. Experimental procedures

2.1. Generation of rdh9-null mice

Rdh9 genomic clones were isolated form a 129SVJ library. The 8-kb genomic fragment with the putative promoter region and exon1 was subcloned into pBSK (Stratagene). A single loxP site was inserted 1660 bp upstream of exon 1, and a neomycin cassette (pGK-Neo) with flanking loxP sites was inserted 330 bp downstream of exon 1. A thymidine kinase cassette (pKO-TK, Stratagene) was cloned into the 3'-end of the targeting vector as a negative selection marker. The targeting construct was linearized with *Not*I and electroporated into E14 embryonic stem cells. After G418 and ganciclovir screening, homologous recombination was confirmed by Southern blotting with two probes: a 5'-probe amplified with 5'-CCAGGGCTGTATCTAGATCCTGCT-3' and 5'-ACAGTACAGGACCCAACATGTCC-3'; and a 3'-probe amplified with 5'-AAACAGTTATTGTTCTAAACTC-3' and 5'-GAACAAGCTGAGTGAGGTGAC-3'. A pCMV-Cre plasmid was introduced into ES clones by electroporation. We used the 5'-probe to identify twenty-seven ES clones with a complete knockout allele by Southern blotting.

Several of these clones were injected into C57BL/6J blastocysts by Chulho Kang (UC-Berkeley Transgenic Facility). Chimeric male mice with a germline knockout allele were mated with C57BL/6J dams. Experiments were done with *rdh9*-mice derived from five backcrosses with C57BL/6J mice, unless noted otherwise.

2.2. Genotyping

Genotyping was done by PCR and/or Southern blotting with tail DNA. PCR samples were lysed overnight at 50°C with proteinase K (5 μl of 10 mg/ml) in 150 μl of 0.45% NP-40 and 0.45% Tween-20 added to an autoclaved buffer of 50 mM KCl, 10 mM Tris, 2 mM $MgCl_2$, 0.1 mg/ml gelatin, pH 8.0. Samples were heated at 95ºC for 10 min and centrifuged (12,000 x *g* for 10 min). We used 1 μl of the supernatant for amplification. The wild-type allele was amplified with forward and reverse primers, 5'-CCCTCTTGAAGTAAGAAGGTA-3' and 5'-ACTCCCAGAGTAGATATGAG-3', respectively, to produce a 1.3 kb product. The null allele was amplified with forward and reverse primers 5'-CCCTCTTGAAGTAAGAAGGTA-3' and 5'-CATTGTTGATGGGATTGCAAGC-3', respectively, to produce a 0.5 kb product. Genomic DNA was prepared with the DNeasy Tissue Kit (Qiagen) and digested with *Eco*RV for Southern blotting. The hybridization probe was the same 5'-probe used for ES cell identification.

2.3. Histology and in situ hybridization

Tissues and embryos were dissected in cold PBS (pH 7.4), fixed in 4% PFA overnight at 4°C, embedded in paraffin, and sliced into 6 μm sections. Slides were stained with hematoxylin and eosin and mounted in Permount (Fisher Scientific). Sections were hybridized overnight at 42° C with a digoxigenin-labeled cRNA probe (Dig RNA labeling kit, Roche; 50 ng labeled probe/slide). The template used to generate the probe was produced by PCR amplifying a section of the 3'-UTR region (forward primer, 5'-AATAGAAATTCCTCTACC-3'; reverse primer, 5'-ATTACTATGCTACGAGAT-3'), and cloning the segment into pBSK. Signals were detected with anti-digoxigenin-AP conjugated Fab fragments and NBT/BCIP tablets (Roche). Light microscopy images (Nikon LABOPHOT-2) were recorded with a SPOT camera (Diagnostic Instruments, Inc).

2.4. RT and real-time quantitative PCR

Total RNA was isolated from tissues or embryos using Trizol reagent (Invitrogen) and was treated with DNase and DNA-free Removal Reagent (Ambion). SuperScript III kit (Invitrogen) and oligo$(dT)_{20}$ were used to reverse transcribe 1.5 μg of RNA. TaqMan real-time quantitative PCR assays were done with a Perkin-Elmer ABI PRISM 7900 sequence detection system, using SDS version 2.0 software (Applied Biosystems). Primers and fluorogenic TaqMan probes were designed with Primer Express software (version 2.0) and synthesized by Applied Biosystems. The comparative Ct method was used to quantify the data. The primers and probes used were (forward primer, reverse primer, probe): *Rdh1*, AAGAGATCTATGGCGAGAAGTTTTTATT, CACAGACAGGTCCTTGTTGCA, 6FAM-TCTATCTGAAAAACCTAAACGAATTGGACA–TAMRA; *Cyp17A1*, GGCTAACATTGACTCCAGCATTG, GTGCCCAGAGATTGATGATCAC, 6FAM-AGTTTGCCATCCCGAAGGACACACA–TAMRA; *Cyp2A5*, TGCGCTATGGCTTTCTGTTG, CACCCGATCAATCTCCTCATG, 6FAM-ATGAAGCACCCAGATATTGAGGCCAAGGT–TAMRA; *3β-HSD2*, CCAGTTTGGGACTGCTGACA, AGTGAGGTTAACTTAATGTACGTGACACT, 6FAM-CACACCCTGTGGCTGACCATCTC–TAMRA; *3β-HSD4*, CTTCCAGACAGACCATCCTAGATGT, TGGCACGTTGGCTTCCA, 6FAM-TCTGAAAGGTACTCAGCTCCTACTGGA–TAMRA; *3β-HSD5*,

GTCGAAAACATGAAGAGGAATTGTC, TCCAGAATGTCTCCCTTCAGTACTC, 6FAM-AAGCTGCAGACAAAGGCCAAGGTG –TAMRA.

2.5. Retinoid analyses

Retinol, RE and RA were quantified as described, with modifications [12]. Briefly, tissues were harvested under yellow light, placed on ice immediately, minced and homogenized in cold phosphate-buffered saline. One ml of 0.025 N KOH/ethanol was added to 0.5 ml of 25% homogenate, followed by extraction with 10 ml hexane. The top (hexane) layer containing retinol and RE was removed and the solvent was evaporated with nitrogen. Residues from kidney, brain, testis, and serum were dissolved in 150 μl acetonitrile. Liver residues were dissolved in 250–500 μl methanol or 500–1000 μl 2-propanol, because of high retinol and RE concentrations. Retinol and RE were resolved by reverse-phase HPLC and quantified by their UV absorbance at 325 nm. The HPLC column was eluted at 1 ml/min with 11% water/methanol for 4.5 min, and then by a linear gradient for 3.5 min to 100% methanol. The 100% methanol wash was maintained for 0.5 min, and then a linear gradient to 5% methanol/95% dichloroethane was generated over 2 min. These conditions were held for an additional 7 min. Retinol eluted at 4.1 ml and RE eluted at 11.4 ml. The injection volume was 100 μl for all samples, with the exception of liver samples for RE analysis. To quantify liver RE accurately a separate 10 μl injection was done. To recover RA, 4 N HCl was added to the aqueous phase (bottom layer) and RA was extracted with another 10 ml of hexane. The solvent was evaporated under a stream of nitrogen and the residues were dissolved in 60 μl of acetonitrile. RA was quantified by a liquid chromatography/tandem mass spectrometry assay [12].

2.6. Microarray analyses

Total RNA was extracted from male mouse livers using Trizol reagent (Invitrogen) and was purified with the Qiagen RNeasy Mini kit. Twenty μg of RNA were reverse-transcribed into amino ally (AA)–dUTP cDNA with the Amersham CyScribe post labeling kit. Cy3 or Cy5 fluorescent dye was incorporated into AA-dUTP cDNA. After purification (Amersham CyScribe GFX kit), labeled cDNA probes were hybridized with glass slide Mouse Exonic Evidence Based Oligonucleotide GeneChips (38,467 oligos) printed in the departmental microarray facility. Dye swap hybridizations were done at 42ºC for 12–16 hr. Chips were scanned with an Applied Precision arrayWoRx scanner. Data analyses were performed using SoftWoRx Tracker version 2.20 (Molecularware, Inc.).

2.7. DHT quantification

DHT was quantified by ELISA (ALPHA Diagnostics International). Briefly, 50 μl of serum were mixed with 100 μl of DHT-horse radish peroxidase conjugate and incubated for 60 min at room temperature with gentle shaking. The buffer was removed and the residue was washed three times with washing buffer. Residues were incubated with horseradish peroxidase substrate solution (150 μl), as supplied by the manufacturer, at room temperature for 15–30 min. Absorbance was measured at 450 nm.

3. Results

3.1. Expression of genes involved in retinoid homeostasis

We determined mRNA levels in mice embryos and embryo livers to place *rdh9* expression into context with genes of retinoid homeostasis (Fig. 1, left). *Rdh9* mRNA expression did not begin in the embryo earlier than e12.5. Thereafter, expression increased, rising sharply from e15.5 to e18.5. Genes encoding other retinol metabolizing enzymes, *rdh6* (Crad1) and *rdh1* (Rdh1), were expressed as early as e7.5, with expression increasing until e18.5 [1,4]. Three genes encoding Raldh were expressed in the embryo as early as e7.5: *Aldh1A1* (Raldh1),

Aldh1A2 (Raldh1), and *Aldh1A3* (Raldh3). A fourth, *Aldh8a1* (Raldh4), began expression on e11.5. *Aldh1a1* expression increased gradually, becoming very intense at later stages of development. *Aldh1a3* expression remained constant from e9.5 through e18.5. The two retinoid catabolic enzymes, *Cyp26A1* and *Cyp26B1* had inversely related expression in the embryo. *Cyp26a1* expression was intense as early as e7.5 and decreased markedly by e11.5. In contrast, intense *Cyp26b1* expression did not begin until e9.5, and thereafter decreased very gradually until e18.5. Detectable expression of *Lrat*, which encodes a retinyl ester-forming enzyme, did not begin until e10.5–e11.5. The retinoid chaperone proteins, CRBPI, CRABPI and CRABPII, were expressed comparatively intensely on e7.5, and the levels remained constant until birth.

Liver was examined because it expresses most, if not all, genes involved in regulating retinoid concentrations, serves as the major organ of retinoid storage, and functions as a major regulator of retinoid homeostasis (Fig. 1, right). *Rdh9* expression began in embryo liver by e13.5, with a marked increase on e16.5, and reached maximum expression after birth by P15. In contrast to the whole embryo, *rdh6* (Crad1) mRNA expression in liver lagged behind *rdh9*, becoming noticeable at birth (P0). Embryonic liver expressed *rdh1*, but expression decreased markedly after P0. Liver expressed *Aldh1a1-3 and Aldh8a1* on e12.5. *Aldh1a3* and *Aldh8a1* expression remained constant from e12.5 to P2M, along with *Rbp1* (CRBPI) and *Lrat* expression. *Aldh1a1* mRNA increased steadily from e12.5 through P2M, and correlated with *rdh9* expression, whereas *Aldh1a2* expression decreased in liver from e12.5 through P2M, and correlated with *rdh1* expression. *Cyp26a1* expression was detected in liver by P2, and increased with time, presumably reflecting accumulation of retinoids. *Cyp26b1* also was detected early and showed a marked increase on P0, which declined abruptly on P22 and continued to decline through P2M. mRNA of the all-trans-RA binding proteins, CRABPI and II, decreased extensively as liver matured: neither were detected on P2.

3.2. Cellular expression of rdh9 during development and postnatally

We next determined *rdh9* expression loci in embryos and adult tissues by in situ hybridization. In the e11.5 embryo, only liver expressed *rdh9*, with even distribution throughout (Fig. 2B, C). Expression increased on e15.5 in liver (Fig. 2D, E). Ganglia (Fig. 2D, F), small intestine (Fig. 2D, H), and developing lung (Fig. 2I) showed weak hybridization signals on e15.5. E16.5 embryos exhibited expression comparable to e15.5 in liver (Fig. 2I-M), and had signals in small intestine, ganglia, and skin. Consistent with the RT-PCR results (Fig. 1B), *rdh9* expression increased markedly in liver on e17.5 compared to e16.5 (Fig. 2N, O), with signals distributed throughout. Expression increased in small intestine (Fig. 2N, 2P), vertebral cartilage (Fig. 2N, 2R), and embryonic lung (Fig. 2N). *Rdh9* was expressed intensely in hepatocytes throughout adult liver (Fig. 3A, B). Convoluted tubules of adult kidney did not express *rdh9*, but glomerulus showed weak signals, whereas collecting tubules produced relatively stronger signals (Fig. 3C, D). The small intestine expressed *rdh9* in glands and throughout the epithelia lining: undifferentiated lining epithelia (close to the submucosa) showed greater expression than differentiated epithelia at the distal end of the villus (Fig. 3E, F). Testis expressed *rdh9* mRNA mainly in spermatogonia, with weaker expression in Leydig cells (Fig. 3G, H). Regions of adult brain that expressed *rdh9* included the dentate gyrus and the CA regions of the hippocampus, the purkinje cells of the cerebellum, and the glomerular and mitral cell layers of the olfactory bulb (Fig. 3I-N).

3.3. Rdh9 ablation

Mouse *rdh9* consists of four exons and spans ~20 kb on chromosome 10D3 [32]. Exon 1 encodes the N-hydrophobic membrane targeting domain, a region crucial for enzymatic activity and direction to the cytosolic face of the endoplasmic reticulum, and the cofactor-binding site [33]. Our targeting vector contained a floxed proximal promoter region and exon 1, followed by a neomycin resistance cassette, ending in a third flox sequence (Fig. 4A). We

used PCR (data not shown) and Southern blotting to confirm homologous recombination (Fig. 4B). Recombinant 129SVJ ES cells were transfected with a pCMV-Cre expression vector. We selected ES cells that had deleted the proximal promoter, exon 1 and the neomycin cassette (Fig. 4C, arrow), or cells that deleted the neocassette, but retained a floxed proximal promoter and exon 1, to generate a conditional knockout, if necessary (Fig. 4C, open arrow). ES cells harboring the complete knockout were injected into blastocysts of C57BL/6 mice. Male chimeras with germline expression were bred with C57BL/6 females to establish strains with a mixed genetic background. Heterozygotes were bred to produce homozygous mice with a hybrid background. Loss of both copies of the wild-type *rdh9* allele was verified by Southern blotting (Fig. 4D) and confirmed by RT-PCR (Fig. 4E) and by in situ hybridization of liver (Fig. 4F).

3.4. Lack of rdh9 does not affect development, viability, or fertility

Rdh9$^{+/-}$ (hybrid background) matings generated pups in Mendelian frequency, confirmed by genotype analysis of 21-day-old mice by PCR and Southern blotting (Table 1). Because a hybrid background sometimes offsets lethal mutations, we backcrossed hybrid background *rdh9*$^{+/-}$ males with C57BL/6 strain females for 5 generations to obtain a genetic background closer to C57BL/6. The offspring bred from the C57BL/6 genetic background mice also were born in Mendelian frequency (Table 1). To evaluate the influence of dietary vitamin A, we reduced the vitamin A from the usual amount in stock chow (>30 IU/g) to 4 IU, the amount of vitamin A recommended for rodent diets by the American Institute of Nutrition [34]. *Rdh9*-null mice fed the lower, but ample amount of vitamin A, also were born in Mendelian frequency (data not shown).

Mice lacking *rdh9* were viable, and their overall appearance was indistinguishable from wild type and heterozygous littermates. We detected no obvious differences in tissue morphology between wild type and null mice in the major sites of *rdh9* expression—liver, kidney, testis, intestine, and brain (Fig. 5). Breeding of male and female *rdh9*-null mice produced normal litter sizes (~6–9 pups/litter) and healthy pups.

3.5. Lack of rdh9 does not affect retinoid levels

We quantified retinoid levels in 22-week-old male mice fed the 4 IU vitamin A/g diet. We detected no significant differences in retinol, RE, and all-trans-RA between wild type and rdh9-null mice in liver, kidney testis, serum, brain and testis (Fig. 6A-C), and did not detect 9-cis-RA in vivo with our liquid chromatography/tandem mass spectrometry assay, which has a lower limit of detection ~5 fmol [12]. Both 13-cis-RA and 9,13-di-cis-RA were present, but both were below limits of quantification (<20 fmol/sample). Younger (6-weeks-old) wild type and null male mice fed diets with 4 or >30 IU vitamin A/g showed no differences in retinoid levels in kidney, serum, brain and testis (data not shown). Retinol and RE concentrations in livers of the younger mice fed the 4 IU vitamin A/g diet were ~25% of the levels in the older mice fed the same diet (Fig. 6D), but there were no significant age-related differences in the other tissues examined (data not shown). Younger mice fed the 30 IU vitamin A/g diet had retinol and RE levels ~8-fold greater than those fed the 4 IU/g diet. Wild type and null female mice also had similar retinoid levels (data not shown).

3.6. Rdh9 deficiency reduces rdh1 mRNA expression

Rdh1 expression decreased markedly in liver, kidney and testis of *rdh9*-null mice relative to wild type mice fed a diet containing >30 IU vitamin A/g (Fig. 7, top). Verification by real-time PCR showed that expression of liver *rdh1* in *rdh9*-null mice decreased by 8-fold (Fig. 7, bottom). Decreased expression of *rdh1* also was observed in *rdh9*-null mice fed a diet with 4 IU vitamin A/g. *Rdh1* expression in the *rdh9*-null mice fed the lower amount of vitamin A,

however, decreased only ~3-fold relative to wild type, i.e. lowering dietary vitamin A increased *rdh1* expression in *rdh9*-null mice, but not in wild-type mice.

We used semi-quantitative PCR to evaluate expression of other genes related to retinoid metabolism or function in heterozygotes and *rdh9*-null mice relative to wild type. Other than Rdh1, enzymes that catalyze retinol dehydrogenation or retinal reduction/dehydrogenation were not affected by the absence of Crad3, including Crad1, Raldh1-4, and Rdh-E_2 (*Dhrs9* or *retSDR8*, also known as hRDH-TBE, h3α-HSD, hRoDH-E_2, and eRolDH) (35–38). The retinoid catabolizing enzymes Cyp26A1 and B1, and the retinoid binding-proteins, CRBPI, CRBPII, CRBPIII and sRBP were not affected. *Lrat* expression did not change in the *rdh9*-null mouse. We noticed no change in the receptors, RARα, β and γ, or in RXRα, β and γ. We noted no changes in Adh1-4 expression.

3.7. Crad3 absence affects expression of Cyp and HSD

We used microarrays to reveal further consequences of nullifying *rdh9*. Total liver RNA samples from 7 to 8-week-old wild type and *rdh9*-null male mice (n = 9, each genotype) fed the 4 IU vitamin A/g diet were divided into 3 equal groups for each genotype, and the mRNAs of each group were combined, yielding three sets of samples for each genotype. Sixty-four genes in the *rdh9*-null mice samples showed 3-fold or greater increases in mRNA, and 44 genes showed 3-fold or greater decreases, relative to wild type (data available on request). Selected results were verified by quantitative real-time RT-PCR (Table 2). Real-time PCR data for the genes selected confirmed the microarray data, with statistically significant differences between the null and wild type mice ($p < 0.05$). Expression decreased of Cyp17A1, the steroid 17α-hydroxylase/17,20-lyase, whereas expression increased of several other enzymes (3β and 17β-HSDs) that catalyze steroid activation and deactivation [39–43]. Three Cyps, which catalyze catabolism of diverse xenobiotics and steroids, also increased in expression: Cyp2A5, 2C29, 3A11 [44–46].

3.8. Rdh9 ablation does not affect serum DHT levels

3α-Dehydrogenation of the weak androgen 3α-androstanediol produces the potent androgen DHT [40,41,43]. *Rdh9*-null mouse serum DHT levels did not differ significantly from wild type (means ± SEM; 223 ± 63 pg/ml, n = 9, and 190 ± 35 pg/ml, n = 10, respectively) (Fig. 8).

4. Discussion

This work was undertaken as part of an effort to provide insight into the function(s) of each gene on mouse chromosome 10D3, which encodes an SDR with activities as retinol and sterol dehydrogenases [32]. These include *rdh9* (Crad3), *rdh1* (Rdh1), *rdh6* (Crad1), *rdh7* (Crad2), *rdh4* (Rdh4), and *rdh8* (17β-HSD9). Of these, Crad3 has the highest efficiency (V_m/K_m) as a 9-cis-retinol dehydrogenase, with Crad1 having ~5-fold less efficiency, Rdh1 having ~10-fold less efficiency, and Crad2 and 17β-HSD9 having negligible activity. Crad3 has ~3-fold greater efficiency for 9-cis-retinol than mouse Rdh4 and its human ortholog Rdh5 [47,48]. Although Rdh4/5 recognize 9-cis-retinol as substrate, they are highly expressed in the eye, where they serve as 11-cis-retinol dehydrogenases: *rdh5* mutations cause the human disease fundus albipunctatus, which involves delayed dark adaptation [49,50]. Crad3 shows no activity with all-trans-retinol, and has ~10-fold less efficiency than Crad1, and 2-fold less efficiency than Rdh1 with 3α-androstandiol. Crad3, therefore, seemed like an attractive candidate for a major 9-cis-retinol dehydrogenase.

The mRNA expression data (Fig. 1) indicate that as early as e7.5 the mouse embryo expresses genes that encode proteins capable of: 1) generating 9-cis-RA (Crad3, Crad1, Rdh1, Raldh1-4); 2) accessing the CRBPI-retinol complex to convert all-trans-retinol into all-trans-RA via all-

trans-retinal (Rdh1; Raldh1-3); 3) modulating all-trans-RA metabolism and delivery to the nucleus (CRABPI, CRABPII) [51,52]. Additionally, beginning with its development, and continuing into the adult, liver expressed the retinol dehydrogenase and Raldh activities necessary and sufficient to convert all-trans- and 9-cis-retinol into all-trans-RA and 9-cis-RA, respectively. Rodents convert exogenous 9-cis-RA rapidly and quantitatively into 9,13-di-cis-RA, and convert 13-cis-RA into 9,13-di-cis-RA, albeit not as efficiently [29,30]. 9,13-di-cis-RA occurs as an endogenous retinoid [29,30]. Therefore, inability to detect 9-cis-RA in vivo does not establish lack of formation.

These mRNA expression results also indicate that quantitatively major RE synthesis does not begin from CRBP-retinol in the embryo until ~e11.5, and RE synthesis does not become robust until ~e16.5. The lack of marked Lrat activity during this period should allow channeling of retinol into RA biosynthesis. The period between e10.5 and e16.5 also lacks intense *Cyp26A1* expression. Lack of *Cyp26A1* expression should result in a longer RA half-life. Decreased *Lrat* and *Cyp26A1* expression, therefore, could increase RA concentrations between e10.5 and e16.5, relative to earlier or latter times.

In situ hybridization (Fig. 2) revealed that early in embryogenesis (e11.5), only liver expressed *rdh9*; other organs (ganglia, small intestine, and skin) did not show intense expression until e16.5. These data also indicated that *rdh9* expression is limited to specific sites of testis, intestine, kidney and brain. All are sites of RXR expression, but RXR expression extends beyond these sites. This distinctive expression pattern suggests Crad3 becomes increasingly important during the later stages of development, serves a specialized purpose in select tissues, and does not serve as a universal producer of an RXR ligand.

Ablating *rdh9* did not have gross effects on retinoid levels in laboratory mice. Nor did fertility or any other obvious retinoid or RXR functions require Crad3 under the conditions tested. This shows only that the laboratory mouse can dispense with Crad3 under controlled conditions. Laboratory mice live in an artificial environment that lacks the stress of living in the wild. As a result of non-natural selection, laboratory mice are larger than wild mice, reach sexual maturity faster, have litters about twice the size of wild mice, and are slower, weaker, and less active. They have smaller brains and lack melatonin [53]. Lack of an astounding phenotype in a laboratory mouse knockout should not be construed as indicating that *rdh9* is not an essential gene.

Ablation of *rdh9* changed the mRNA expression levels of enzymes involved in steroid homeostasis. Expression of *Cyp17A1* decreased—a gene that encodes the steroid 17α-hydroxylase/17,20-lyase, crucial for biosynthesis of estrogen and androgens. Increases were noted in expression of several enzymes (3β and 17β HSDs) that catalyze steroid activation or deactivation, downstream of the 17α-hydroxylase/17,20-lyase [40–43]. Three Cyps (Cyp2A5, 2C29, 3A11), which catabolize steroids and function downstream of the HSDs, also increased in expression [44–46]. These data indicate that *rdh9* nullification disrupts steroid homeostasis. The lack of change in serum DHT, a major product of Crad3 in vitro, could reflect the occurrence of many enzymes with 3α-adiol dehydrogenase activity, and compensatory changes in response to loss of Crad3. On the other hand, the Cyp2A, 2C, and 3A families are well known for substrate promiscuity. For example, Cyp3A4, the human homolog of mouse Cyp3A11, accounts for ~30% of the total liver Cyp content, and metabolizes fatty acids, prostaglandins, fat-soluble vitamins and up to 60% of prescription drugs, in addition to natural and synthetic steroids [44,45]. Their lack of substrate discrimination makes changes in Cyp2A5, 2C29, and 3A11 difficult to interpret.

We determined expression levels of *Adh1-4*, because these non-specific, xenobiotic metabolizing enzymes recognize retinol in vitro [54–56]. Gene knockouts, however, do not

provide support for Adh metabolizing retinoids under physiological conditions, as no *Adh*-null mice have phenotypes related to retinoid function, or show compensatory expression changes in genes that encode proteins involved in retinoid metabolism or function [57,58]. To date the only data consistent with Adh metabolizing retinol in vivo have been generated with a single extraordinarily high dose (50 mg/kg), which would overcome controls imposed by retinoid binding proteins [57]. Because CRBP prevents Adh from metabolizing retinol [59,60], using such an overwhelming dose does not provide physiological, or even universal pharmacological insight. The present data also are non-informative about a putative function for Adh in retinol metabolism.

This work did not reveal lack of RXR function or disturbances in retinoid metabolism in the *rdh9*-null mouse, despite our previous demonstration that Crad3 functions in intact cells in a reconstituted system (Crad3 plus Raldh) to produce 9-cis-RA from 9-cis-retinol [2]. This does not exclude Crad3 functioning as a 9-cis-retinol dehydrogenase in vivo, because other SDR, including Crad1 and Rdh1, also recognize 9-cis-retinol as substrate, albeit ~10-fold less efficiently than Crad3. Alternatively, Crad3 may function in androgen metabolism—a function also potentially hidden through compensation by numerous enzymes, but suggested here by changes in Cyp and HSD expression.

Acknowledgements

This work was supported by Public Health Service Grants DK36870 and DK29644 from the National Institutes of Diabetes, Digestive and Kidney diseases.

References

1. Napoli JL. 17β-Hydroxysteroid dehydrogenase type 9 and other short-chain dehydrogenases/reductases that catalyze retinoid, 17β- and 3α-hydroxysteroid metabolism. Mol Cell Endocrinol 2001;171:103–109. [PubMed: 11165018]
2. Zhuang R, Lin M, Napoli JL. Cis-retinol/androgen dehydrogenase, isozyme 3 (Crad3): a short-chain dehydrogenase active in a reconstituted path of 9-*cis*-retinoic acid biosynthesis in intact cells. Biochemistry 2002;41:3477–3483. [PubMed: 11876656]
3. El Alkawi Z, Napoli JL. Rat liver cytosolic retinal dehydrogenase: comparison of 13-*cis*-, 9-*cis*-, and all-*trans*-retinal as substrates and effects of cellular retinoid-binding proteins and retinoic acid on activity. Biochemistry 1994;33:1938–1943. [PubMed: 8110799]
4. Napoli JL. Interactions of retinoid binding proteins and enzymes in retinoid metabolism. Biochim Biophys Acta 1999;1440:139–162. [PubMed: 10521699]
5. Lin M, Napoli JL. cDNA cloning and expression of a human aldehyde dehydrogenase (ALDH) active with 9-cis-retinal and identification of a rat ortholog, ALDH12. J Biol Chem 2000;275:40106–40112. [PubMed: 11007799]
6. Laudet V. Evolution of the nuclear receptor superfamily: early diversification from an ancestral orphan receptor. J Mol Endocrinol 1997;19:207–226. [PubMed: 9460643]
7. Mark M, Ghyselinck ND, Chambon P. Function of retinoid nuclear receptors: lessons from genetic and pharmacological dissections of the retinoic acid signaling pathway during mouse embryogenesis. Annu Rev Pharmacol Toxicol 2006;46:451–480. [PubMed: 16402912]
8. Szantol A, Narkar V, Shen Q, Uray IP, Davies PJA, Nagy L. Retinoid X receptors: X-ploring their (patho)physiological functions. Cell Death Differen 2004;11:S126–S143.
9. Heyman RA, Mangelsdörf DJ, Dyck JA, Stein RB, Eichele G, Evans RM, Thaller C. 9-cis-Retinoic acid is a high affinity ligand for the retinoid X receptor. Cell 1992;68:397–406. [PubMed: 1310260]
10. Levin AA, Sturzenbecker LJ, Kazmer S, Bosakowski T, Huselton C, Allenby G, Speck J, Kratzeisen C, Rosenberger M, Lovey A. 9-cis-Stereoisomer of retinoic acid binds and activates the nuclear receptor RXRα. Nature 1992;355:359–361. [PubMed: 1309942]
11. Schmidt CK, Brouwer A, Nau H. Chromatographic analysis of endogenous retinoids in tissues and serum. Anal Biochem 2003;315:36–48. [PubMed: 12672410]

12. Kane MA, Chen N, Sparks S, Napoli JL. Quantification of endogenous retinoic acid in limited biological samples by LC/MS/MS. Biochem J 2005;388:363–369. [PubMed: 15628969]
13. de Urquiza AM, Liu A, Sjöberg M, Zetterstrom RH, Giffiths W, Sjövall J, Perlmann T. Docosahexaenoic acid, a ligand for the retinoid X receptor in mouse brain. Science 2000;290:2140–2144. [PubMed: 11118147]
14. Kitareewan S, Burka L, Tomer B, Parker CE, Deterding LJ, Stevens RD, Forman BM, Mais DE, Heyman RA, McMorris T, Weinberger C. Phytol metabolites are circulating dietary factors that activate the nuclear receptor RXR. Mol Cell Biol 1999;7:1153–1166.
15. LeMotte PK, Keidek S, Apfel CM. Phytanic acid is a retinoid X receptor ligand. Eur J Biochem 1996;236:328–333. [PubMed: 8617282]
16. Bourguet W, Vivat V, Wurtz JM, Chambon P, Gronemeyer H, Moras D. Crystal structure of a heterodimeric complex of RAR and RXR ligand-binding domains. Mol Cell 2000;5:289–298. [PubMed: 10882070]
17. Brown PS, Blum WP, Stern WH. Isomers of vitamin A in fish liver oils. Nature 1959;184:1377–1379. [PubMed: 13804998]
18. Bushway RJ. Separation of carotenoids in fruits and vegetables by high performance liquid chromatography. J Liq Chrom 1985;8:1527–1547.
19. Chandler GW, Schwartz SJ. HPLC separation of cis-trans carotene isomers in fresh and processed fruits and vegetables. J Food Sci 1987;52:669–672.
20. Schwartz SJ. Chromatographic analysis of cis/trans carotenoid isomers. J Chrom 1992;624:235–252.
21. Levin G, Mokady S. 9-cis-β-carotene as a precursor of retinol isomers in chicks. Int J Vitam Nutr Res 1994;64:165–169. [PubMed: 7814229]
22. Pott I, Marx M, Neidhart S, Muhbauer W, Carle R. Quantitative determination of β-carotene stereoisomers in fresh, dried, and solar-dried mangoes (Mangifera indica L.). J Agric Food Chem 2003;51:4527–4531. [PubMed: 14705872]
23. Dew SE, Ong DE. Specificity of the retinol transporter of the rat small intestine brush border. Biochemistry 1994;33:12340–12345. [PubMed: 7918456]
24. Stahl W, Schwarz W, Sundquist AR, Sies H. Cis-trans isomers of lycopene and β-carotene in human serum and tissues. Arch Biochem Biophys 1992;294:173–177. [PubMed: 1550343]
25. Stahl W, Sundquist AR, Hanusch M, Schwarz SW, Sies H. Separation of β-carotene and lycopene geometric isomers in biological samples. Clin Chem 1993;39:1810–814.
26. Yeum KJ, Booth SL, Sadowski JA, Liu C, Tang G, Krinsky NI, Russell RM. Human plasma carotenoid response to the ingestion of controlled diets high in fruits and vegetable. Am J Clin Nutr 1996;64:594–602. [PubMed: 8839505]
27. Clinton SK, Emenhiser C, Schwartz SJ, Bostwick DG, Williams AW, Moore BJ, Erdman JW. cis-trans Lycopene isomers, carotenoids, and retinol in the human prostate. Can Epidem Biomark Prevent 1996;5:823–833.
28. Tzimas G, Sass JO, Wittfoht W, Elmazar MM, Ehlers K, Nau H. Identification of 9,13-dicis-retinoic acid as a major plasma metabolite of 9-cis-retinoic acid and limited transfer of 9-cis-retinoic acid and 9,13-dicis-retinoic acid to the mouse and rat embryos. Drug Metab Dispos 1994;22:928–936. [PubMed: 7895612]
29. Horst RL, Reinhardt TA, Goff JP, Nonnecke BJ, Gambhir VK, Fiorella PD, Napoli JL. Identification of 9,13-di-cis-retinoic acid as a major circulating retinoid in plasma. Biochemistry 1995;34:1203–1209. [PubMed: 7827070]
30. Horst RL, Reinhardt TA, Goff JP, Koszewski NA, Napoli JL. 9,13-di-cis-Retinoic acid is the major circulating geometric isomer of retinoic acid during the periparturient period. Arch Biochem Biophys 1995;322:235–239. [PubMed: 7574681]
31. Sass JO, Tzimas G, Elmazar MM, Nau H. Metabolism of retinaldehyde isomers in pregnant rats: 13-*cis*- and all-*trans*-retinaldehyde, but not 9-cis-retinaldehyde, yield very similar patterns of retinoid metabolites. Drug Metab Dispos 1999;27:317–321. [PubMed: 10064560]
32. Zhang M, Thomas BC, Napoli JL. Gene structure and minimal promoter of mouse *rdh1*. Gene 2003;305:121–131. [PubMed: 12594048]
33. Zhang M, Hu P, Napoli JL. Elements in the N-terminal signaling sequence that determine cytosolic topology of short-chain dehydrogenases/reductases: studies with retinol dehydrogenase type 1 and

cis-retinol/androgen dehydrogenase type 1. J Biol Chem 2004;279:51482–51489. [PubMed: 15355969]

34. Reeves PG. Components of the AIN-93 diets as improvements in the AIN-76A diet. J Nutr 1997;127:838S–841S. [PubMed: 9164249]
35. Chetyrkin SV, Belyaeva OV, Gough WH, Kedishvili NY. NY Characterization of a novel type of human microsomal 3α-hydroxysteroid dehydrogenase: unique tissue distribution and catalytic properties. J Biol Chem 2001;276:22278–22286. [PubMed: 11294878]
36. Soref CM, Di YP, Hayden L, Zhao YH, Satre MA, Wu R. Characterization of a novel airway epithelial cell-specific short chain alcohol dehydrogenase/reductase gene whose expression is up-regulated by retinoids and is involved in the metabolism of retinol. J Biol Chem 2001;276:24194–24202. [PubMed: 11304534]
37. Markova NG, Pinkas-Sarafova A, Karaman-Jurukovska N, Jurukovski V, Simon M. Expression pattern and biochemical characteristics of a major epidermal retinol dehydrogenase. Mol Genet Metab 2003;78:119–135. [PubMed: 12618084]
38. Rexer BN, Ong DE. A novel short-chain alcohol dehydrogenase from rats with retinol dehydrogenase activity, cyclically expressed in uterine epithelium. Biol Reprod 2002;67:1555–1564. [PubMed: 12390888]
39. Hall PF. Cytochromes P450 and regulation of steroid synthesis. Steroids 1986;48:131–196. [PubMed: 3328326]
40. Mahendroo MS, Cala KM, Russell DW. 5α-Reduced androgens play a key role in murine parturition. Mol Endocrinol 1996;10:380–392. [PubMed: 8721983]
41. Payne AH, Hales DB. Overview of steroidogenic enzymes in the pathway from cholesterol to active steroid hormones. Endocrine Rev 2004;25:947–970. [PubMed: 15583024]
42. Simard J, Ricketts M, Gingras S, Soucy P, Feltus FA, Melner MH. Molecular biology of the 3β-hydroxysteroid dehydrogenase/Δ^5-Δ^4 isomerase gene family. Endocrine Rev 2005;26:525–582. [PubMed: 15632317]
43. Miller WL. Androgen biosynthesis from cholesterol to DHEA. Mol Cell Endocrinol 2002;198:7–14. [PubMed: 12573809]
44. Guengerich FP. Cytochrome P-4503A4: regulation and role in drug metabolism. Annu Rev Pharmacol Toxicol 1999;39:1–17. [PubMed: 10331074]
45. Goodwin B, Redinbo MR, Kliewer SA. Regulation of CYP3A gene transcription by the pregnane X receptor. Annu Rev Pharmacol Toxicol 2002;42:1–23. [PubMed: 11807162]
46. Passcussi JM, Gerbal-Chaloin S, Drocourt L, Maurel P, Vilaren MJ. The expression of CYP2B6, CYP2C9 and CYP3A4 genes: a tangle of networks of nuclear and steroid receptors. Biochim Biophys Acta 2003;1619:243–253. [PubMed: 12573484]
47. Driessen CAGG, Winkens HJ, Kuhlmann ED, Janssen APM, van Vugt AHM, Deutman AF, Janssen JJM. The visual cycle retinol dehydrogenase: possible involvement in the 9-cis-retinoic acid biosynthetic pathway. FEBS Letters 1998;428:135–140. [PubMed: 9654122]
48. Wang J, Chai X, Eriksson U, Napoli JL. Activity of human Rdh5 with steroids and retinoids and expression of its mRNA in extra-ocular human tissue. Biochem J 1999;338:23–27. [PubMed: 9931293]
49. Jang GF, van Hooser JP, Kuksa V, McBee JK, He YG, Janssen JJ, Driessen CA, Palczewski K. Characterization of a dehydrogenase activity responsible for oxidation of 11-cis-retinol in the retinal pigment epithelium of mice with a disrupted RDH5 gene, A model for the human hereditary disease fundus albipunctatus. J Biol Chem 2001;276:32456–32465. [PubMed: 11418621]
50. Liden M, Romert A, Tryggvason K, Persson B, Eriksson U. Biochemical defects in 11-cis-retinol dehydrogenase mutants associated with fundus albipunctatus. J Biol Chem 2001;276:49251–49257. [PubMed: 11675386]
51. Fiorella PD, Napoli JL. Microsomal retinoic acid metabolism: effects of cellular retinoic acid-binding protein (type I) and C18-hydroxylation as an initial step. J Biol Chem 1994;269:10538–10544. [PubMed: 8144640]
52. Sessler RJ, Noy N. A ligand-activated nuclear localization signal in cellular retinoic acid binding protein-II. Mol Cell 2005;18:343–353. [PubMed: 15866176]

53. Miller RA, Harper JM, Dysko RC, Durkee SJ, Austad SN. Longer life spans and delayed maturation in wild-derived mice. Exp Biol Med 2002;227:500–508.

54. Pares X, Julia P. Isoenzymes of alcohol dehydrogenase in retinoid metabolism. Methods Enzymol 1990;189:436–441. [PubMed: 2292955]

55. Yang ZN, Davis GJ, Hurley TD, Stone CL, Li TK, Bosron WF. Catalytic efficiency of human alcohol dehydrogenases for retinol oxidation and retinal reduction. Alcohol Clin Exp Res 1994;18:587–591. [PubMed: 7943659]

56. Martas S, Alvarez R, Martinez SE, Torres D, Gallego O, Duester G, Farres J, de Lera AR, Pares X. The specificity of alcohol dehydrogenase with cis-retinoids: activity with 11-cis-retinol and localization in retina. Eur J Biochem 2004;271:1660–1670. [PubMed: 15096205]

57. Deltour L, Foglio MH, Duester G. Metabolic deficiencies in alcohol dehydrogenase Adh1, Adh3, and Adh4 null mutant mice. Overlapping roles of Adh1 and Adh4 in ethanol clearance and metabolism of retinol to retinoic acid. J Biol Chem 1999;274:16796–16801. [PubMed: 10358022]

58. Molotov A, Fan X, Deltour L, Foglio MH, Martras S, Farres J, Pares X, Duester G. Stimulation of retinoic acid production and growth by ubiquitously expressed alcohol dehydrogenase Adh3. Proc Natl Acad Sci USA 2002;99:5337–5342. [PubMed: 11959987]

59. Boerman MHEM, Napoli JL. Cellular retinol-binding protein-supported retinoic acid synthesis: relative roles of microsomes and cytosol. J Biol Chem 1996;271:5610–5616. [PubMed: 8621422]

60. Kedishvili NY, Gough WH, Davis WI, Parsons S, Li TK, Bosron WF. Effect of cellular retinol-binding protein on retinol oxidation by human class IV retinol/alcohol dehydrogenase and inhibition by ethanol. Biochem Biophys Res Commun 1998;249:191–196. [PubMed: 9705855]

Abbreviations

Adh
: alcohol dehydrogenase

Crad
: *cis*-retinoid androgen dehydrogenase

DHT
: dihydrotestosterone

HPLC
: high-performance liquid chromatography

HSD
: hydroxysteroid dehydrogenase

Raldh
: retinal dehydrogenase

RA
: retinoic acid

RE
: retinyl ester

SDR
: short-chain dehydrogenase/reductase

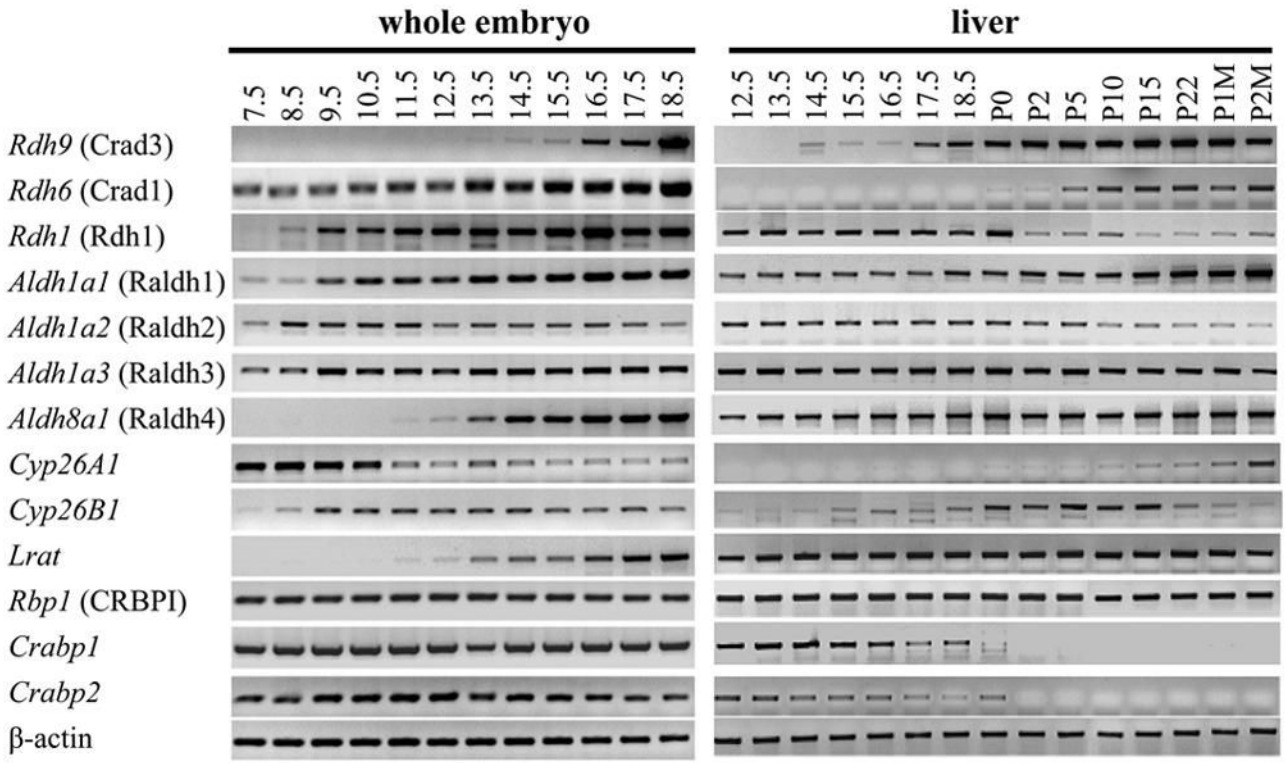

Figure 1.

Rdh9 (Crad3) mRNA expression during embryo and liver development relative to genes related to retinoid homeostasis. Left) RT-PCR was done with gene-specific primers with RNA from embryos ($n \geq 3$ at each stage). Cycles used were: *rdh9* (Crad3), *rdh6* (Crad1), *rdh1* (Rdh1), 40*; Crabp1 & 2*, 35*; actin*, 25; all others, 30. Right) RT-PCR was done with liver RNA from embryos (e12.5 to e18.5) and pups (P0 to P2M) ($n = 3$). Cycles used were: *rdh9* (Crad3), *rdh6* (Crad1), *Aldh1a1* (Raldh1), *Aldh8a1* (Raldh4), *Lrat, Rbp1* (CRBPI), 30*; rdh1* (Rdh1), *Aldh1a2* (Raldh2), *Aldh1a3* (Raldh3), *Cyp26A1*, *Cyp26B1*, *Crabp1 & 2*, 35; *actin*, 25.

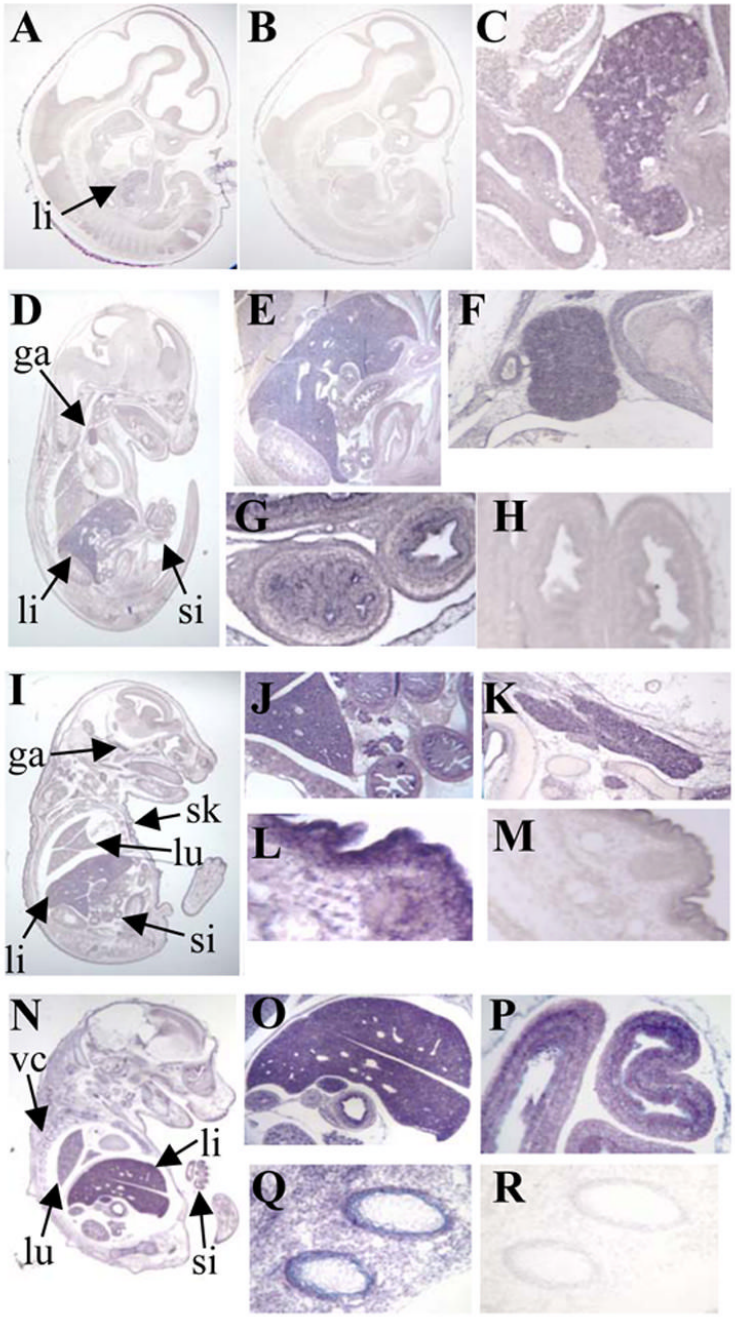

Figure 2.

Rdh9 mRNA expression during development. In situ hybridization was done on parasagittal sections of staged embryos with digoxigenin-labeled cRNA. A) Expression on e11.5 was detected only in liver; B) sense probe control; C) higher magnification of region (arrow) in A showing expression throughout liver. D) Expression on e15.5 was detected in liver (li), ganglia (ga), and small intestine (si). E, F, H) Higher magnifications of liver, ganglia, and small intestine, respectively, denoted by arrows in D. H) Sense probe control of small intestine. I) *Rdh9* expression on e16.5 in liver, ganglia, small intestine, lung (lu) and skin (sk). J, K, L) Higher magnifications of liver and small intestine, ganglia, and skin, respectively, denoted by arrows in I. M) Sense probe control of skin. N) Expression on e17.5 in liver, lung, small

intestine, and vertebral cartilage (vc). O, P, Q) Higher magnifications of liver, small intestine, and vertebral cartilage, respectively. R) Sense probe of vertebral cartilage. Images A, B, D, I, and N, 10X; others, 40X.

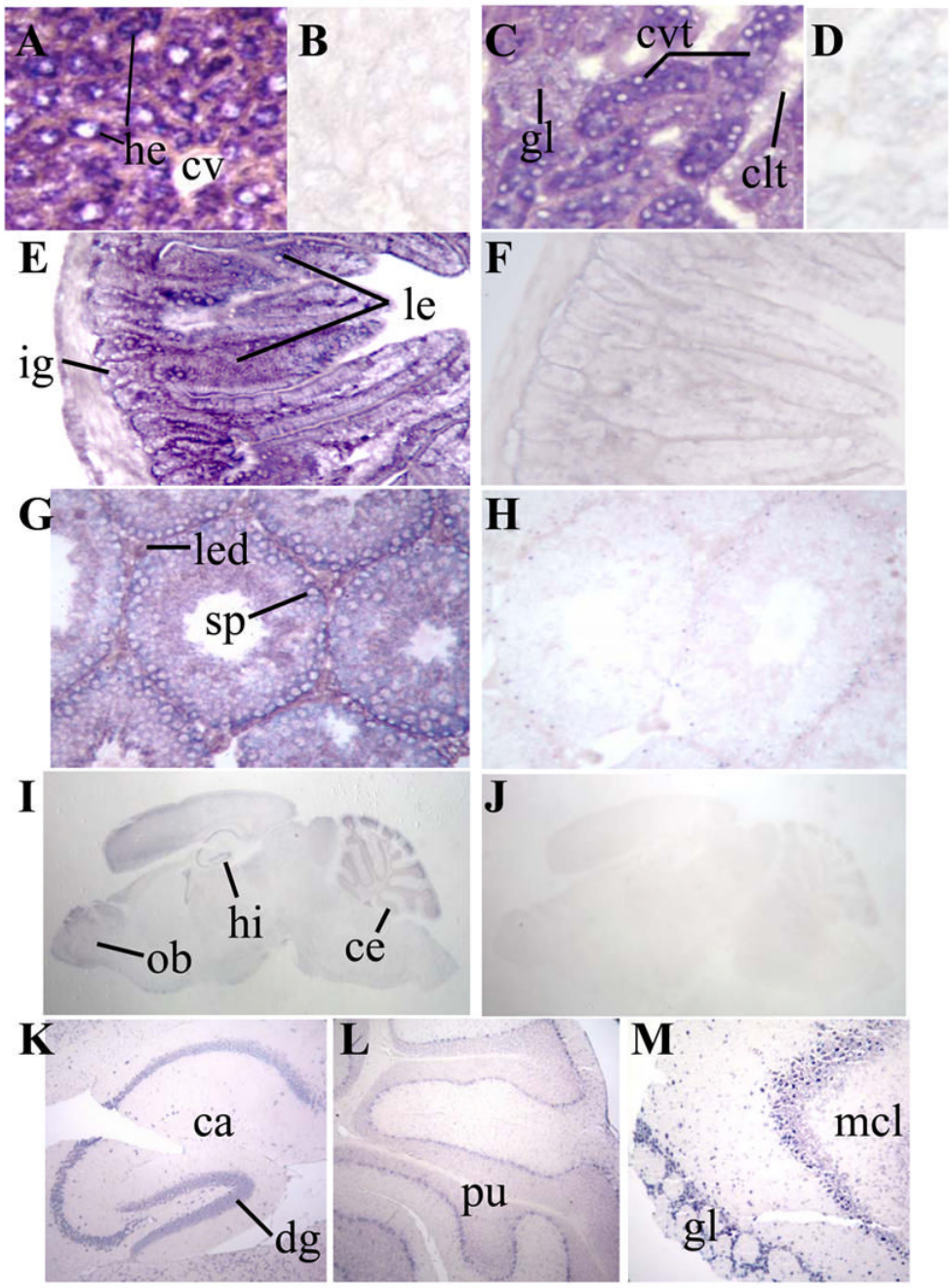

Figure 3.

Expression of *rdh9* mRNA in adult tissues. In situ hybridization was done with antisense (A, C, E, G, I, and K-M) and sense (B, D, F, H, and J) probes. A, B) Liver, showing extranuclear expression in hepatocytes (he) and not in the central vein (cv). C, D) Kidney, showing expression in convoluted tubules (cvt), but not in collecting tubules (clt), with glomerulus (gl) showing weak expression. E, F) Small intestine showing expression in the glands (ig) and throughout the lining epithelia (le). G, H) Testis expression was confined to spermatogonia (sp), with weaker expression in Leydig cells (led). I, J) Expression in the adult brain occurred in the hippocampus (hi), olfactory bulb (ob), and cerebellum (ce). L, M, N) Higher magnifications of the expressing regions of I. K) Expression in the dentate gyrus (dg) and CA

regions of the hippocampus. L) Cerebellum expression localized to purkinje cells (pu). M) The mitral cell layer (mcl) and glomerular layer (gl) expressed *rdh9* mRNA.

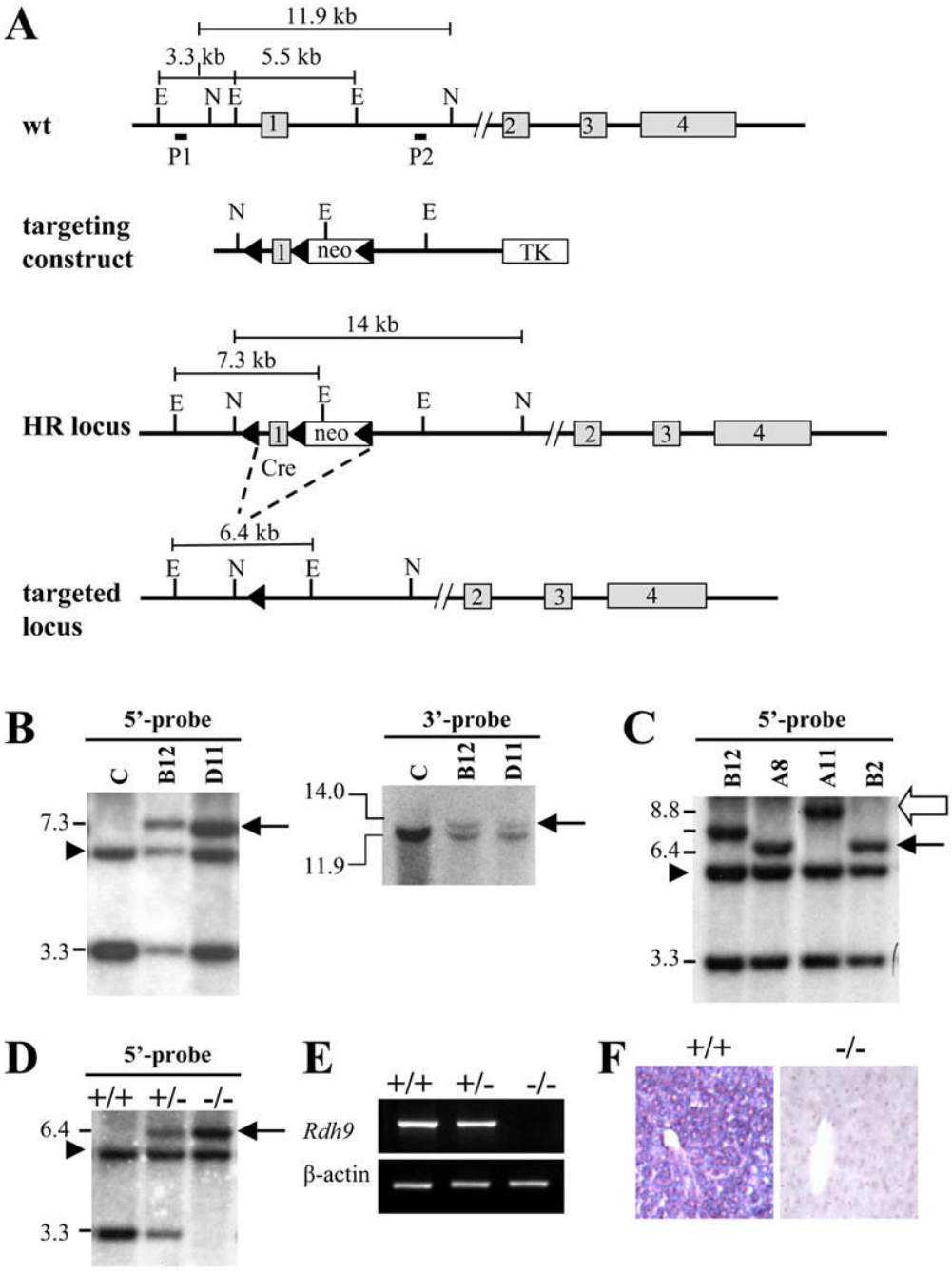

Figure 4.

Targeted disruption of *rdh9.* A) The top line shows a partial restriction map of mouse *rdh9,* which consists of 4 exons spanning ~20 kb on chromosome 10D3. Probe locations: P1, 5' probe; P2, 3'-probe. N and E, *Nde*I and *Eco*RI sites, respectively, The targeting construct contained a floxed PGK-neo selection cassette inserted into intron 1, a single LoxP site inserted before the proximal promoter, and a thymidine kinase (TK) negative selection marker at the 3'-end. The homologous recombination (HR) locus shows integration of the targeting vector into the genome. The genomic region between the first and the third LoxP sites was removed by expression of pCMV-Cre in ES cells with HR. B) Homologous recombination between the targeting construct and the wild-type locus was identified by Southern blotting with probes P1

and P2. Arrows show hybridization bands indicating HR. C) Probe P1 was used to identify the null allele in Cre-expressing ES cells by Southern blotting. The solid arrow shows a band indicating the null allele. The open arrow shows a band indicating a conditional knockout allele, in which deletion occurred between the LoxP sites flanking the PGK-neo cassette. B, C) The arrowheads show a nonspecific band. D) Southern blotting verified *rdh9* null mice. A 6.4 kb band (arrow) indicated the null allele; a ~3.3 kb band indicated the wild type allele. E, F) RT-PCR and in situ hybridization in liver confirmed loss of *rdh9* null mice.

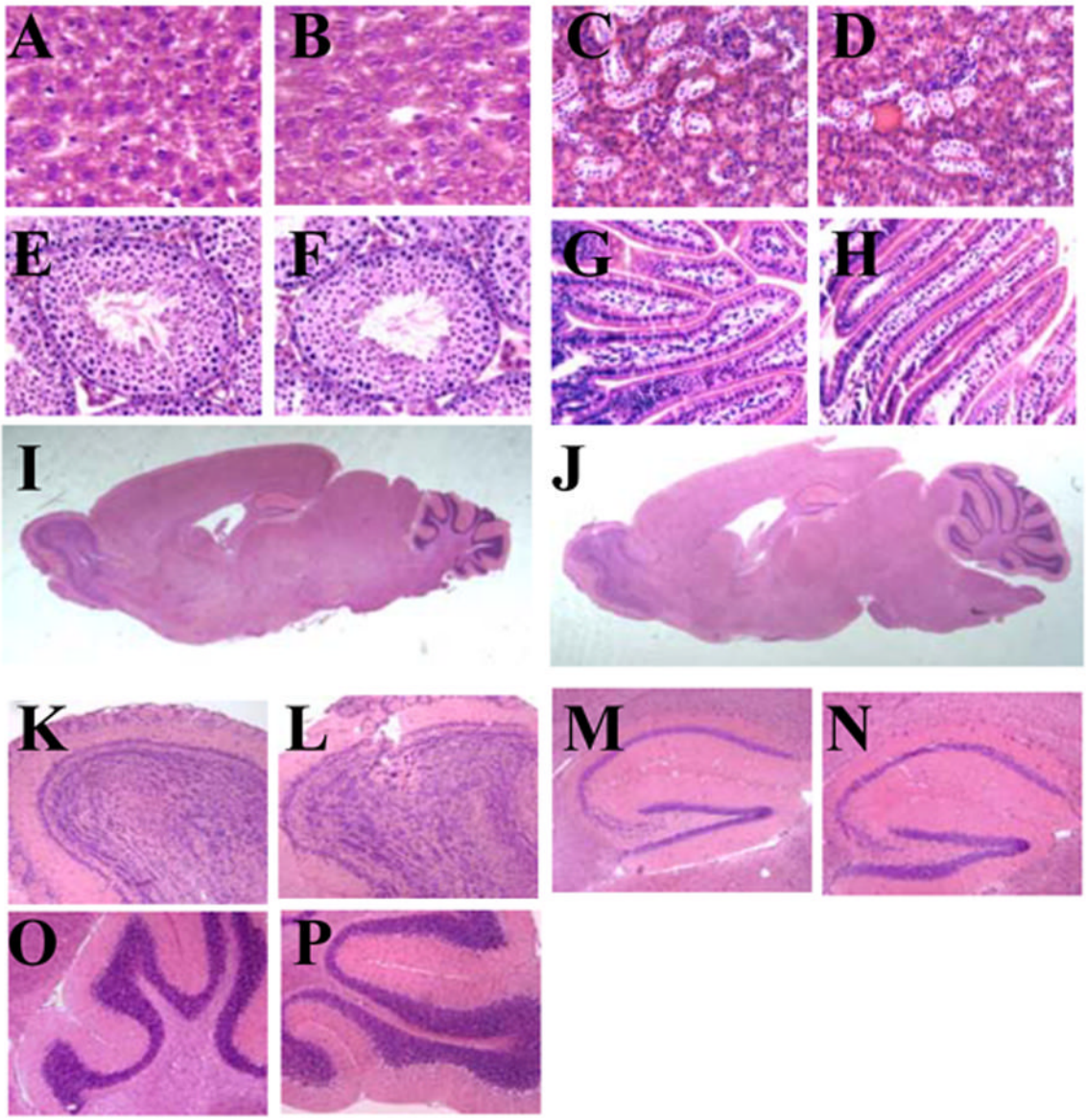

Figure 5.
Morphology of *rdh9* null mice. A, C, E, G, I, K, M, O) Wild-type tissues. B, D, F, H, J, L, N, P) Tissues from null mice. A, B) Liver. C, D) Kidney. E, F) Testis. G, H) Small intestine. I, J) Brain. K, L) Olfactory bulb. M, N) Hippocampus. O, P) Cerebellum. Tissues were stained with H & E.

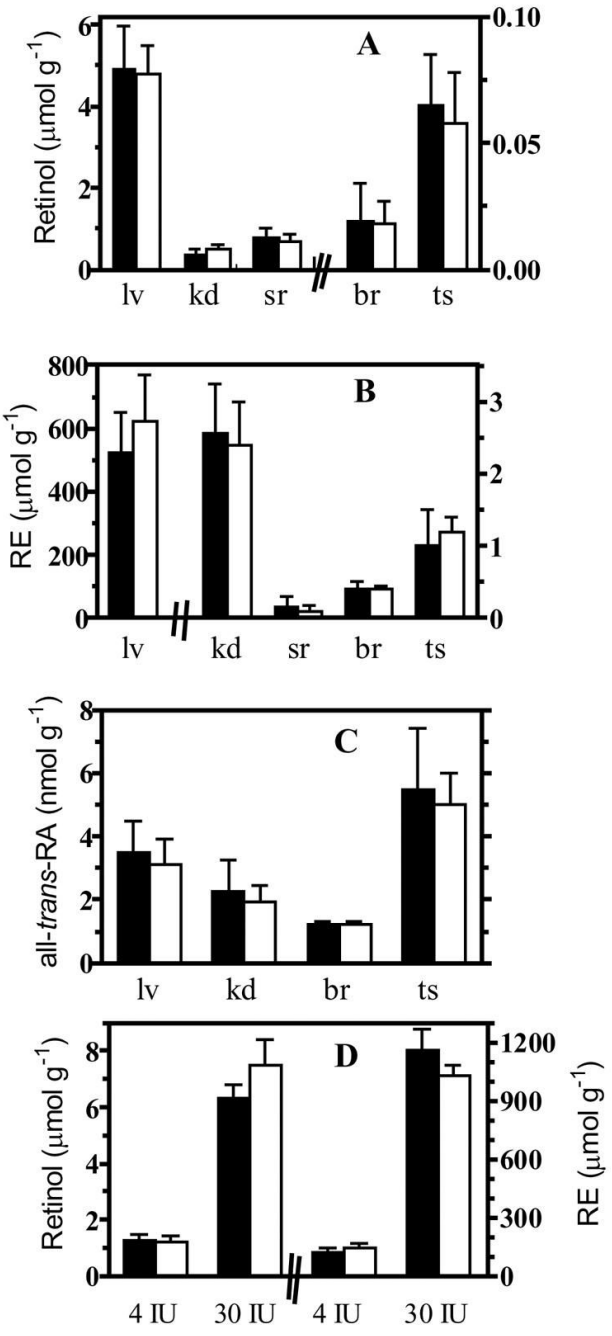

Figure 6.

Retinoid status in *rdh9*-null mice. Tissues were harvested from male mice fed a 4 IU vitamin A/g diet since birth (22 weeks total): A) retinol, B) RE, C) all-trans-RA. Bars to the left of the breaks relate to the left Y-axis scale and bars to the right of the breaks relate to the right Y-axis scale: lv, liver; kd, kidney; sr, serum; br, brain; ts, testis. D) Mice were fed a 4 IU vitamin A/g or >30 IU vitamin A/g diet since birth (total 6 weeks). Bars to the left of the break show retinol values and bars to the right of the break show RE values. Retinol and its esters were quantified by HPLC. RA was quantified by LC/MS/MS. Filled bars, wild type; open bars, *rdh9*-null. Data are means ± SD, n = 4–8.

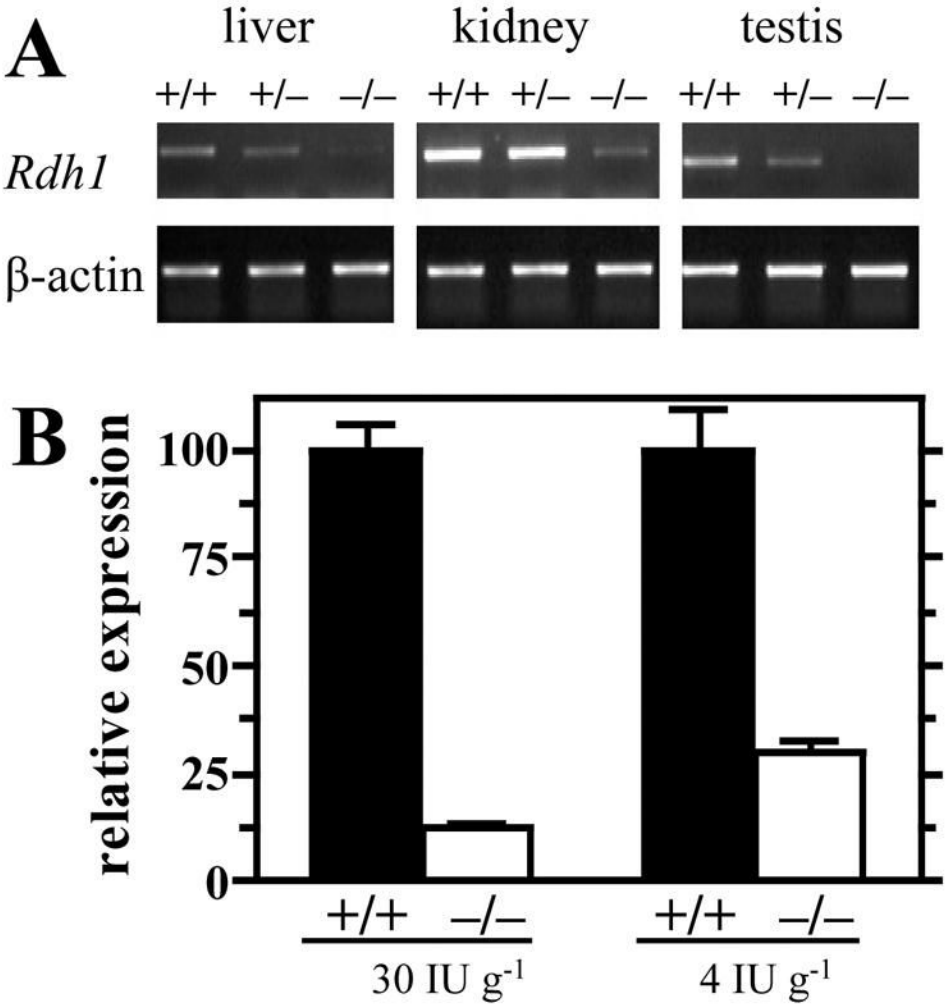

Figure 7.

Decreased expression of *rdh1* mRNA in tissues of *rdh9*-null mice. A) Semi-quantitative RT-PCR (35 cycles with 1.5 μg RNA) showed a decrease in *rdh1* expression in homozygous knockout tissues. B) *Rdh1* mRNA in liver was quantified by real-time quantitative PCR. *Rdh1* mRNA expression in wild type (filled bars) vs. null-mice (open bars) fed a diet containing >30 IU vitamin A/g. Lowering total dietary vitamin A to 4 IU/g did not affect expression in wild-type liver, but caused a 2-fold increase in null liver, resulting in a difference between wild-type and null of ~3-fold. Data are normalized to expression in wt mice fed the diet with >30 IU vitamin A/g. *Rdh1* mRNA expression in *rdh9*-null mice fed the two diets differed significantly from each other, and from expression in wild type mice: **p* <0.002, n = 8, means ± SD.

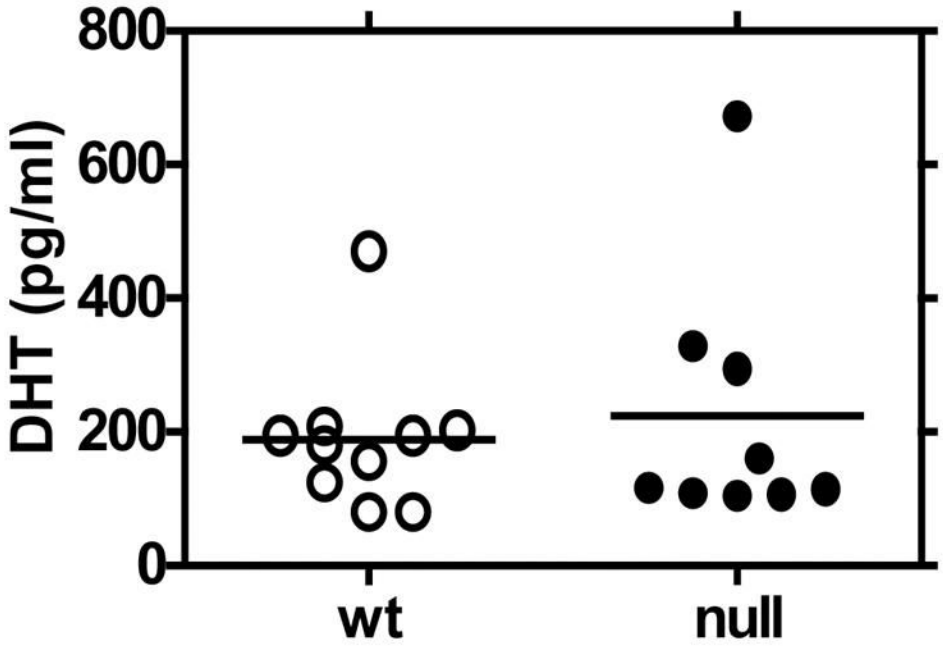

Figure 8.
DHT levels of *rdh9*-null mice. Serum from three-month-old male mice (wild-type, n = 10, open circles; *rdh9*-null, n = 9, filled circles) was assayed by ELISA for DHT.

TABLE 1

Offspring of *rdh9*$^{+/-}$ breeding conform to Mendelian ratios

genotype	Before backcross[a]		After backcross[b]	
	No. of mice	% total	No. of mice	% total
+/+	49 (24 ♂ + 25 ♀)	28	62 (32 ♂ + 30 ♀)	24
+/–	80 (35 ♂ + 45 ♀)	46	120 (53 ♂ + 67 ♀)	47
–/–	46 (24 ♂ + 22 ♀)	26	75 (34 ♂ + 41 ♀)	29

[a] F1 generation.

[b] Five backcrosses against a C57BL/6 background.

TABLE 2

Gene expression changes in *rdh9*-null mouse liver

Gen Bank accession No.	Gene	Fold change		Function
		microarray	Q-PCR	
NM_007809	CYP17A1	−3	−2	Biosynthesis of DHEA and androstenedione
NM_007812	CYP2A5	+4	+2	Xenobiotic and steroid metabolism
NM_007815	CYP2C29	+3	--	Xenobiotic and steroid metabolism
NM_007818	CYP3A11	+5	--	Xenobiotic and steroid metabolism
NM_153193	3βHSD2	+4	+3	Steroid hormone biosynthesis
NM_008295	3βHSD4	+4	+2	3-Ketosteroid reductases, inactivation of sterioid hormones, such as DHT
NM_008294	3βHSD5	+3	+2	
NM_013786	17β-HSD9	+3	--	Dehydrogenation of DHT, E_2, 3α-adiol
NM_080436	mRDH1	ND[1]	−3	Dehydrogenation of all-*trans*-retinol, 9-*cis*-retinol, 3α-adiol

[1] ND, not detected.